ELSEVIER

Earth and Planetary Science Letters 175 (2000) 169–180

EPSL

www.elsevier.com/locate/epsl

The intensity of the time-averaged geomagnetic field: the last 5 Myr

M.T. Juarez [a], L. Tauxe [b,*]

[a] *Fort Hoofddijk Paleomagnetic Laboratory, Budapestlaan 17, 3584 CD Utrecht, The Netherlands*
[b] *Scripps Institution of Oceanography, La Jolla, CA 92093-0220, USA*

Received 27 September 1999; received in revised form 29 November 1999; accepted 29 November 1999

Abstract

The existing database for paleointensity estimates of the ancient geomagnetic field contains more than 1500 data points collected through decades of effort. Despite the huge amount of work put into obtaining these data, there remains a strong bias in the age and global distribution of the data toward very young results from a few locations. Also, few of the data meet strict criteria for reliability and most are of unknown quality. In order to improve the age and spatial distribution of the paleointensity database, we have carried out paleointensity experiments on submarine basaltic glasses from a number of DSDP sites. Of particular interest are the sites that provide paleointensity data spanning the time period 0.3–5 Ma, a time of relatively few high quality published data points. Our new data are concordant with contemporaneous data from the published literature that meet minimum acceptance criteria, and the combined data set yields an average dipole moment of $5.49 \pm 2.36 \times 10^{22}$ Am^2. This average value is comparable to the average paleofield for the period 5–160 Ma ($4.2 \pm 2.3 \times 10^{22}$ Am^2) [T. Juarez, L. Tauxe, J.S. Gee and T. Pick (1998) Nature 394, 878–881] and is substantially less than the value of approximately 8×10^{22} Am^2 often quoted for the last 5 Myr (e.g. [McFadden and McElhinny (1982) J. Geomagn. Geoelectr. 34, 163–189; A.T. Goguitchaichvili, M. Prévot and P. Camps (1999) Earth Planet. Sci. Lett. 167, 15–34]).

Keywords: magnetic intensity; paleointensity; magnetic field; paleomagnetism; secular variations

1. Introduction

Coe [4] was one of the first to estimate the average strength of the geomagnetic field. Based on the paleointensity data available in 1967, he suggested that the average field was approximately 60% of the present geomagnetic field strength. In terms of the axial dipole moment, this would have been $\sim 5 \times 10^{22}$ Am^2. Using a larger data set, McFadden and McElhinny [2] estimated an average dipole moment of the geomagnetic field of approximately $8.67 \pm 0.65 \times 10^{22}$ Am^2 [2], comparable to the present geomagnetic axial dipole (7.8×10^{22} Am^2 [5]). This larger estimate of average value has remained essentially unchallenged in the intervening decades (see e.g. [3]).

Several indirect lines of evidence point to a time-averaged geomagnetic field strength that is

* Corresponding author. Tel.: +1-858-534-6084; Fax: +1-858-534-0784; E-mail: ltauxe@ucsd.edu

0012-821X/00/$ – see front matter
PII: S0012-821X(99)00306-4

closer to Coe's original estimate. Gee et al. [6] showed that sedimentary paleointensity records for the Brunhes, when cross-calibrated with absolute paleointensity estimates, yield an average dipole moment for the Brunhes that is lower than that of the present field, a contention they support with an interpretation of marine magnetic anomalies. The relative paleointensity data set of Valet and Meynadier [7] which spans the last 4 million years was similarly cross-calibrated and yields an estimate for the average dipole moment of $4.2 \pm 2.1 \times 10^{22}$ Am^2. Numerical simulations of geomagnetic field using the method described by Glatzmaier and Roberts (e.g. [8]) generally have average values that are lower than the present geomagnetic field [9]. Finally, the average value of the Cenozoic and late Mesozoic has recently been shown to be half that of the present field [1]. These indirect clues hint that the average field during the so-called 'Mesozoic dipole low' [10] was perhaps closer to the time-averaged value of the geomagnetic field than is the present dipole moment.

In this paper, we discuss the absolute paleointensity database for the last 5 Myr. Because most of the data come from the last few hundred thousand years, and the recent field may have been unusually strong, we consider only those data older than 0.3 Ma. We will also present new data derived from paleointensity experiments of submarine basaltic glass (SBG) for this time period. These combined data sets will be used to address the issue of the strength of the time-averaged geomagnetic field.

2. Published database

The availability of reliable absolute paleointensity data is quite restricted. Recent studies (e.g. [3]) have shown conclusively that the best method for obtaining such data is that of Thellier–Thellier with the inclusion of so-called pTRM checks [11] (here called T+; see in addition e.g. [4,12,13]). Other methods have more limited means of assessing data reliability. The complete T+ experiment is difficult and extremely time consuming. Because of this, most of the published data are based on quicker methods and may be of lower quality.

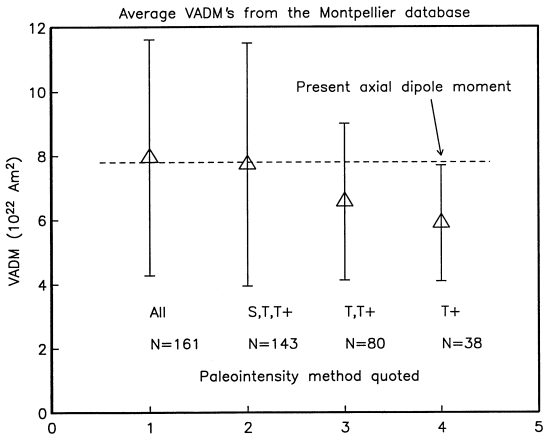

Fig. 1. Dependence of average VADM estimates on the method used to generate paleointensity data. 'S' is Shaw method [16], 'T' is Thellier–Thellier [11], and 'T+' is Thellier–Thellier plus pTRM checks (see text). Methods with more reliability checks reduce the estimate significantly. The most reliable method (T+) results in an average significantly different from the present field. These data are listed in Table 1.

Because of the scarcity of high quality paleointensity data, most attempts to estimate the average field have tended to include more data of lesser quality in the hope of averaging out random noise. The bias introduced by including data of unknown quality may not be random and their inclusion could result in estimated field values that are seriously in error.

The effect of using data of questionable quality is illustrated in Fig. 1. We begin with the most recent available compilation of paleointensity [14] from: ftp://ftp.dsdu.univ-montp2.fr/pub/paleointdb.

The so-called 'Montpellier 1998' database was trimmed as follows:

- We extracted all data in the range of 0.3–5 Ma as this range corresponds to the new data presented later in this paper. Exclusion of the most recent data also counteracts the bias introduced by the preponderance of very young data in the database which may be sampling high fields.
- Because there has been inordinate interest in abnormal field behavior associated with polar-

Table 1
Data from the Montpellier data base selected as described in the text

Unit	λ/ϕ	Age (Ma)	N	B	VADM	Ref.
1356	38.14/140.46	1	2	33.90 ± 3.9	5.99	[23]
1357	38.14/140.46	1	5	32.40 ± 4.9	5.72	[23]
1382	50.26/6.71	0.4 ± 0.4	5	22.10 ± 1.7	3.43	[24]
1383	50.24/6.71	0.4 ± 0.4	6	52.20 ± 3.4	8.11	[24]
1386	50.08/7.02	0.4 ± 0.4	7	53.50 ± 7.8	8.32	[24]
1387	50.25/6.78	0.4 ± 0.4	5	49.70 ± 4.3	7.72	[24]
1388	50.15/6.81	0.4 ± 0.4	5	40.80 ± 2.6	6.34	[24]
1389	50.15/6.81	0.4 ± 0.4	7	39.50 ± 2.9	6.14	[24]
1391	50.24/6.74	0.4 ± 0.4	5	26.40 ± 1	4.10	[24]
1392	50.08/7.02	0.4 ± 0.4	6	62.00 ± 2.7	9.64	[24]
1393	50.18/6.60	0.4 ± 0.4	6	15.50 ± 1.7	2.41	[24]
1395	50.21/6.77	0.4 ± 0.4	5	11.10 ± 0.7	1.72	[24]
1396	50.26/6.73	0.4 ± 0.4	5	29.10 ± 2.1	4.52	[24]
1397	50.24/6.67	0.4 ± 0.4	5	28.40 ± 3.7	4.41	[24]
1400	50.21/6.67	0.4 ± 0.4	6	33.60 ± 2	5.22	[24]
1402	50.08/6.78	0.4 ± 0.4	11	44.10 ± 3.9	6.86	[24]
1403	50.08/6.78	0.4 ± 0.4	6	55.60 ± 5.3	8.65	[24]
1405	50.15/6.98	0.4 ± 0.4	11	48.70 ± 5.3	7.57	[24]
1406	50.20/6.77	0.55 ± 0.03	5	43.60 ± 3.1	6.77	[24]
1408	50.28/6.63	0.55 ± 0.4	5	33.60 ± 1.4	5.22	[24]
1409	50.28/6.56	0.55 ± 0.4	5	41.30 ± 2.7	6.41	[24]
1410	50.11/6.93	0.55 ± 0.4	6	34.50 ± 3.5	5.36	[24]
1412	50.29/6.66	0.48 ± 0.03	5	26.90 ± 3	4.18	[24]
1413	50.26/6.79	0.4 ± 0.4	11	49.60 ± 4.3	7.70	[24]
1415	50.16/6.81	0.51 ± 0.03	6	30.40 ± 2.6	4.72	[24]
1416	50.11/6.93	0.4 ± 0.4	11	47.10 ± 6	7.32	[24]
1417	50.26/6.66	0.4 ± 0.4	5	54.40 ± 2.9	8.45	[24]
1418	50.43/7.14	0.4 ± 0.4	9	29.10 ± 2.5	4.51	[25]
1419	50.42/7.1	0.4 ± 0.4	5	31.00 ± 3.2	4.81	[25]
1471	50.34/7.2	0.4 ± 0.4	15	45.30 ± 4.4	7.03	[26]
1472	50.47/7.3	0.366 ± 0.04	6	29.40 ± 1.3	4.56	[26]
1473	50.47/7.3	0.491 ± 0.08	6	41.60 ± 4.1	6.45	[26]
1474	50.45/7.1	0.47 ± 0.05	3	50.50 ± 4.9	7.83	[26]
1475	50.37/7.3	0.35 ± 0.05	6	51.10 ± 1.8	7.93	[26]
1478	50.43/7.2	0.42 ± 0.03	7	43.40 ± 3.2	6.73	[26]
1487	50.35/7.2	0.41 ± 0.03	7	32.60 ± 3.8	5.06	[26]
1495	64.40/−21.5	2.58 ± 0.2	2	26.60 ± 0.5	3.71	[21]
1498	64.40/−21.5	2.58 ± 0.2	4	32.10 ± 3.8	4.48	[21]

Unit is the REFNO from the database. λ is latitude and ϕ is longitude. N is the number of samples used to calculate a cooling unit average. B is the paleofield estimate. VADM is the VADM in units of 10^{22} Am^2 calculated from B and λ. Ref. is the reference.

ity transitions and there is the likelihood of unusually low fields associated with transitions, we have excluded all results designated as transitional in the database.

- We remove all data from cooling units with uncertainties (defined by the standard deviation over the mean) greater than 15%.
- Finally, we calculated a virtual axial dipole moment (VADM) by:

$$\mathrm{VADM} = \frac{4\pi r^3}{\mu_o} B(1 + 3\cos^2\lambda)^{-1/2} q$$

where r is the average value of the Earth's radius

and μ_o is the permeability of free space (see e.g. [15]), B is the paleofield estimate and λ is the present site latitude. This of course assumes that plate motion has been negligible (less than a few degrees) in the last five million years.

There are 161 paleofield estimates meeting these minimum criteria obtained using a variety of paleointensity techniques. The arithmetic mean VADM is 7.95 ± 3.67 (all VADM values are given in units of 10^{22} Am^2). The value of the axial dipole of the geomagnetic reference field (IGRF 1995 [5]) is 7.8. These results suggest that the present field is of average intensity. When we exclude all methods other than the 'Shaw' method (S, [16]) and various forms of the 'Thellier–Thellier' (T, [11]), there are 143 data points with an average VADM of 7.73 ± 3.78. Further restricting the data to Thellier–Thellier only, there are 80 data points with an average of 6.75 ± 2.44. Finally, if only Thellier–Thellier data generated using the so-called 'pTRM checks' (T+) are selected, there are only 38 data points with an average of 5.9 ± 1.8, significantly different from the present axial dipole.

The T+ data from the Montpellier database meeting the minimum criteria discussed above are listed in Table 1. They come from only three locations and are concentrated in the last one million year interval. The question arises whether the average value of the geomagnetic field calculated from these 38 cooling units is representative of the time-averaged field, or whether it is affected by the limited temporal and spatial sampling of the cooling units. In order to address the issue of spatial and temporal sampling of the time-averaged geomagnetic field, we have focussed on the SBG collection of the Deep Sea Drilling Project (DSDP). In this paper, we present new data spanning the critical interval 0.3–5 Ma obtained from SBG. The resulting database, while still incomplete, has improved spatial and temporal sampling and may therefore yield a more realistic estimate of the time-averaged paleointensity for the last 5 Myr.

Table 2
Locations of DSDP sites used in this study

Site	Age (Ma)	λ/ϕ
482	0.3	22.8/−108
483	2	22.9/−108.7
474	3.1	23/−109
420	3.4	9/−106
332	3.9	36.9/−33.6

3. Sample distribution, and ages and experimental aspects

We sampled all sites from DSDP drill cores with ages less than five million years that recovered basaltic glass. Sites that gave interpretable results are listed along with their ages and present locations in Table 2. We estimate ages based on the marine magnetic anomaly pattern as correlated with the geomagnetic polarity time scale [17]; these are accurate to within approximately 0.1 Myr. Sites can be back-tracked to their original paleolatitudes if the site location, tectonic plate, and age are known and some plate motion model is assumed. In fact, there has been very little plate motion for most of these young sites; present latitudes are all within a degree or two of their formation latitudes and we simply use the present latitudes for the VADM calculations.

The depth distribution of specimens resulting in a successful paleointensity experiment are listed in Table 3. While specimens from Site 332 span a large range of depths and are likely to span tens of thousands of years or more, other sites (e.g. 474) have a very narrow depth range and are likely to sample a short amount of time. Unfortunately, there is no way to estimate accurately the time span over which flows from a given drill core accumulated.

The chips that we obtained are small, weighing between 0.1 and 0.5 g, and were peeled from the margins of pillows. These were first measured with a 2G cryogenic magnetometer at the 'Fort Hoofddijk' paleomagnetic laboratory in order to select samples of sufficient magnetization to carry out the paleointensity experiment. Only chips with natural remanent magnetizations (NRMs) of at least 10^{-9} Am^2 were used in our study. This criterion excluded some 90% of the glass samples

that were obtained. Low intensities of NRM, along with the widespread superparamagnetic and paramagnetic behavior observed in our SBG specimens stems from the extremely small grain size of the magnetites and their very low abundance (see [18]).

The chips that met the intensity requirements were cleaned in 1.7 N HCl for approximately 5 min in order to remove surface contamination. Every chip was pressed into a 1.2 cm diameter-0.9 cm height cylinder of reagent grade NaCl in order to facilitate orientation during the experiment and to reduce alteration in atmosphere during heating.

The paleointensity experiments were carried out in the Scripps Paleomagnetic Laboratory. Remanence measurements were made on a CTF cryogenic magnetometer. The experimental design we used to determine the paleointensity at each site is based on the stepwise double heating method of Thellier and Thellier [11], as modified by Coe [12]. Experimental details are described more fully in [19]. Each specimen was heated twice at 50° intervals from 100° to 300° and at 25° intervals thereafter until the noise level of the magnetometer or the maximum unblocking temperature of the specimen was reached.

The first heating and cooling cycle was done in zero field and the second was done in a laboratory field (B_{lab}) of 30 μT, applied along the axis of the salt cylinders. Every 100°, a lower temperature in-field step was repeated after the zero field step. This procedure, first suggested by the Thellier's themselves [11], is termed the 'pTRM check' (e.g. [13]) and is useful for determining whether the specimen has begun to undergo chemical alteration that affects its ability to acquire a thermal remanence. The pTRM checks provide a necessary but not sufficient test for the reliability of the data.

We use five criteria to evaluate the quality of our paleointensity data. These are similar to those used by [19] although we have modified the details somewhat:

(1) The data are plotted as NRM intensity remaining after each zero field step against the pTRM acquired in the in-field step (see Fig. 2a,c,e). The scatter about the best-fit line is given by the standard error of the slope (σ) over the absolute value of the slope ($|b|$) [13]. (The pTRM checks are not included in the calculation of the slope or scatter). Based on visual inspection of many such plots, we chose an arbitrary value of 0.1 as a maximum acceptable value scatter for a minimum of four consecutive temperature steps. This is termed the 'scatter criterion'.

(2) A comparison of pTRM checks with the original pTRM value is an indication of either poor reproducibility (usually accompanied by large scatter), or alteration of the remanence carrying capacity of the specimen. We calculate the difference between the two in-field measurements at a given step. It is common practice to constrain repeat values of two in-field measurements to agree within 5% (see e.g. [19]). This biases against the lower temperature steps as the pTRM acquired is rather small, so reproducibility to a given percentage is more difficult to achieve. We have considered a number of possible approaches to quantifying the degree of difference between the two pTRM measurements and find that all have drawbacks. After careful consideration, we normalize the difference between the two repeat pTRM steps by the length of the line through the data points used in the slope calculation. This has the effect of penalizing results based on a small fraction of the NRM, a desirable result. We express the difference ratio (DRAT) as a percentage. A DRAT of less than 10% was chosen as the maximum acceptable for the 'DRAT criterion'.

(3) We plot the zero field steps as vector endpoint diagrams (see Fig. 2b,d,f). (Please note that the specimens are unoriented geographically). The cylinder axis is labelled 'Z' and an arbitrary fiducial axis on the top of the cylinder is treated as 'X'. The laboratory field was applied along 'Z' and the data are plotted with the X–Y data pairs as solid symbols and the X–Z data pairs as open symbols. The principal components calculated through the same data points as used for the NRM-pTRM slope calculation (solid symbols in Fig. 2a,c,e) are shown as heavy dashed lines. The principal components are calculated along with the maximum angular deviation (MAD) using the method of Kirschvink [20]. The MAD is a qualitative indication of scatter about the best-fit

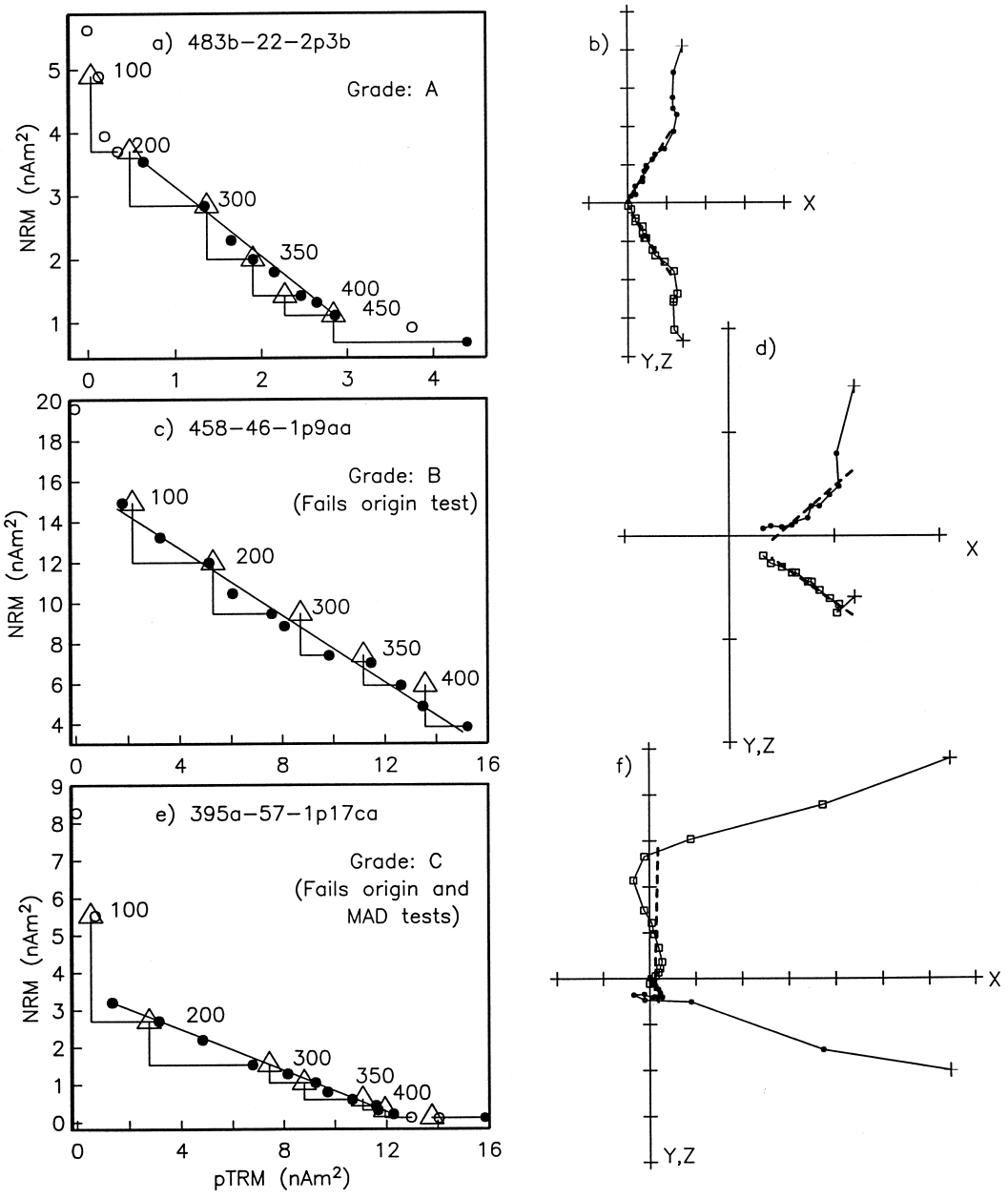

Fig. 2. Representative behavior of specimens during the Thellier–Thellier experiment. a, c and e are Arai plots of NRM remaining against pTRM gained at each temperature step. Solid symbols are data points used in the slope calculation. Triangles are the repeated pTRM steps (the pTRM checks) performed after the zero field step indicated by the right hand end-point of the right angle. b, d and f are vector end-point diagrams of the zero field steps. Solid symbols are X,Y (in specimen coordinates) and open symbols are X,Z, where Z is the axis along the length of the cylindrical specimens and X is an arbitrary fiducial line on the top of the specimens. (a,b) Representative grade A specimen. (c,d) Grade B specimen that fails the origin test, but otherwise would be acceptable. (e,f) Grade C specimen that fails both the MAD and origin tests, clearly displaying a complicated remanence which would be accepted on the basis of the Arai plot alone.

line. A maximum value of MAD was taken to be 15° and constitutes the 'MAD criterion'. Most of our results have much lower MAD values as high MAD values tend to be accompanied by other inadequacies in the data (for example, high scatter).

(4) In order to insure that the data used for the slope calculation belonged to the characteristic component (and not some viscous or component of unknown origin), we check to make sure that the principal component trends toward the origin (see also [19]). This is done by comparing the direction of the vector average of the data (which are anchored to the origin) with the principal component (which are anchored to the 'center of mass' of the data) using the zero field measurements for the data used in the slope calculation. The angle between these two vectors (α) must be less than 10°. This is termed 'the origin criterion'.

If the first four criteria are met, the specimen is given a grade of 'A'. Grade 'B' data pass three of the four and grade 'C' pass only two. Grades 'D' and 'F' pass one and no criteria, respectively. In Fig. 2a,b, we show a representative example of a grade 'A' result. In Fig. 2c,d, we show an example of data from a specimen that would ordinarily be deemed acceptable for paleointensity studies that do not consider the origin test (the scatter and DRAT criteria are met). When plotted as NRM remaining versus pTRM gained, the data appear to be reasonably well behaved, but the principal component bypasses the origin by a significant amount. Hence, the component that would be chosen for paleointensity analysis is not the characteristic component. It is therefore unlikely that this component is the original TRM and its origin is unknown. We have observed that the slope calculated through data not belonging to the characteristic component but some viscous component, is much steeper than the slope corresponding to the characteristic component when the polarity is the same as the present field (by far the majority of the data in the published literature). Without considering the origin test, the characteristic component may actually be avoided because of the onset of alteration as evidenced by the pTRM checks. Thus the temptation is strong to select the lower temperature steps because the pTRM checks are good, while ignoring the fact that the data may not belong to the original TRM. Paleofield estimates derived from such data are more often than not biased too high.

The data in Fig. 2e also would appear reasonable without consideration of the behavior of the zero field steps shown in Fig. 2f. These data reveal that the specimen has a complicated demagnetization behavior resulting from several overlapping components of NRM. Data from specimens such as this are eliminated by the MAD and origin criteria.

We list in Table 3 the grade 'A' results of our T+ experiments from sites whose ages fall within the last five million years. The specimen names (*xxx*[a–d]-*yy*-*z*p*n*[a–b]) provide the key to where in the drill core the specimen was taken. The hole is designated by *xxx*[a–d]. The core by *yy* and the section by *z*. The depth to the top of the core section is also given in Table 3. In DSDP drill cores, each piece of continuous core material is numbered and the piece number is given by p*n* in the specimen name. Multiple specimens from the same piece are designated by us as a, b, etc. Usually, multiple specimens from the same piece can be considered replicates from the same cooling unit. In some cases, pieces were broken but could be fit together by DSDP staff. In such cases, pieces were labelled, for example p8a, p8b. For these, we use a double letter for the specimen designation (aa, ab, ba, bb). In these cases (e.g. 483-23-1p8aa and ab in Table 3), 'aa' and 'ba' would be the 'a' specimens from subpieces. A complete list of data (including all the 'failed' results) can be obtained by anonymous ftp at: ftp://sorcerer.ucsd.edu/pub/data/sbg98.

Although there are many reliability checks in the T+ experiment, it is nonetheless still possible for a specimen to achieve a grade of 'A' and yet yield an entirely erroneous result. For example, the salt from which the specimen pellet was made could have been contaminated with some magnetic material or the glass chip itself could have a spurious magnetization due to alteration of the magnetic phase on the sea floor or remagnetization by subsequent lava flows. Although not often observed in the glass data, the Arai plots

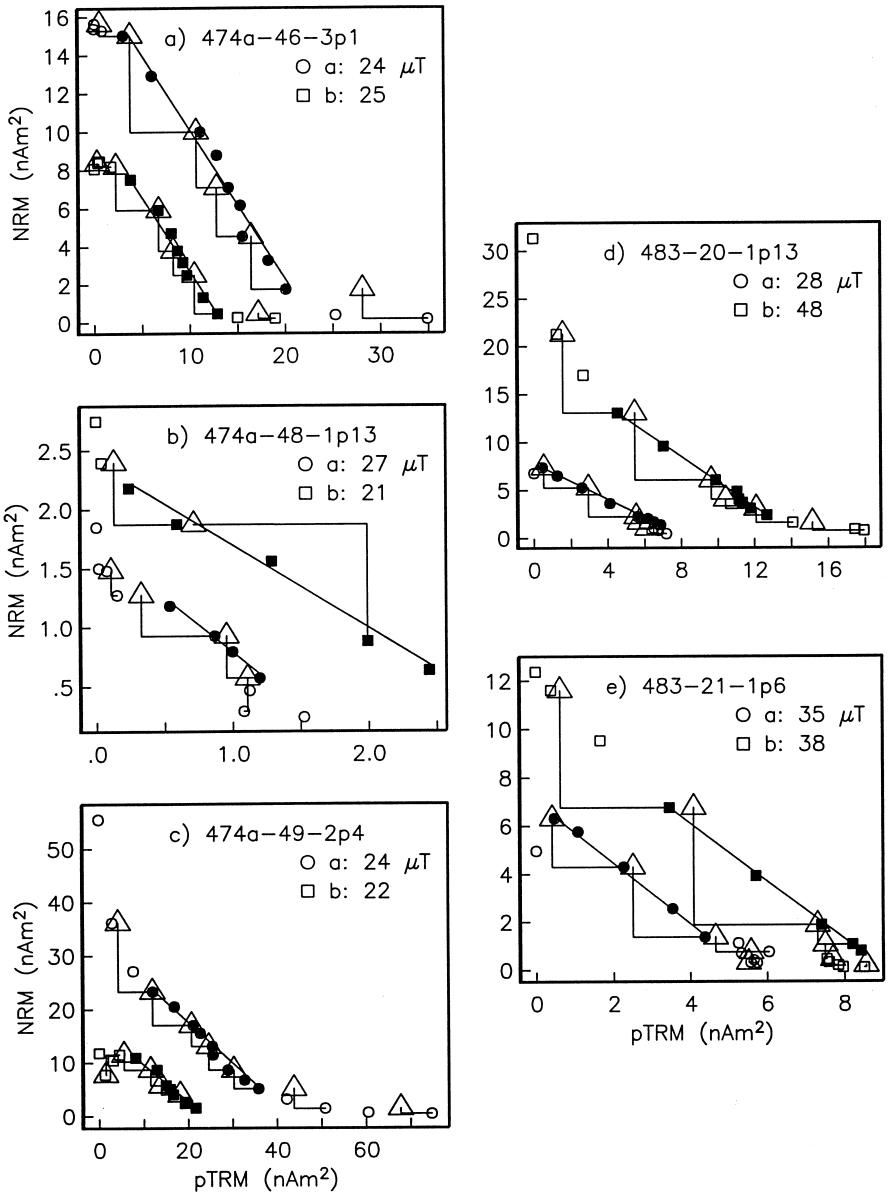

Fig. 3. Arai plots from specimen pairs from the same chilled margin. Symbols as in Fig. 2. The intensities of specimens 483-20-1p13a and 483-21-1p6b were reduced by a factor of 10 for purposes of plot clarity. The field estimates calculated for all specimens are listed in the figure notes. In general, the estimates agree very well, with (d) illustrating the exception.

could be curved owing to the presence of multidomain grains (an effect first discussed by Coe [4]). In such cases, selection of the wrong part of the curve will yield the wrong answer.

Because spurious magnetizations may not be detected through the first four criteria, a useful fifth criterion would be agreement between multiple chips obtained from the same glassy margin. Unfortunately, it is often not possible to obtain duplicate specimens from the DSDP core material. Nonetheless, whenever possible, we measured a second specimen from what appeared to be the

Table 3
All grade A specimens considered for this study

Specimen	Depth	T_{min}–T_{max}	N	B (μT)	Q	σ/|b|	MAD	α	DRAT	VADM
332a-22-1p2a	254	100–450	11	17	57.1	0.015	3.6	3.1	4.5	3.05
332a-26-1p5b	292	100–450	11	15	24.3	0.028	11.8	4.2	10.5	2.69
332a-8-1p7b	121	150–325	5	27	8.8	0.027	15.9	15.2	2.1	4.85
332b-48-1p6b	712	100–450	11	21	20.1	0.038	7.4	1.6	10.0	3.77
420-14-1p1a	118	150–375	7	12	13.4	0.040	2.2	2.1	7.8	3.0
*420-17-1p1a	141.5	100–400	9	14	11.9	0.065	3.8	3.1	6.6	3.50
474a-46-3p1a	584	200–450	9	24	10.9	0.058	4.7	4.6	5.8	5.15
474a-46-3p1b	584	250–450	8	25	9.0	0.059	5.7	1.9	6.7	5.36
474a-47-3p1b	593	250–425	7	23	4.5	0.080	5.8	2.2	6.5	4.93
474a-48-1p13a	599	250–350	4	27	3.3	0.070	3.8	6.5	9.6	5.79
474a-48-1p13b	599	150–325	5	21	7.1	0.065	11.3	4.3	4.6	4.50
*474a-48-3p1b	602	240–450	8	20	6.7	0.082	11.4	9.0	6.3	4.29
*474a-49-1p1a	608	200–350	5	13	11.5	0.022	10.2	10.6	10.0	2.79
474a-49-2p4a	609.5	200–450	9	24	9.2	0.051	11.5	11.0	4.0	5.15
474a-49-2p4b	609.5	250–450	7	22	5.0	0.085	4.1	3.3	9.3	4.72
482d-11-2p4b	161	100–300	5	13	10.5	0.047	8.1	5.9	10.3	2.79
482d-11-3p3ab	161	150–400	8	35	6.7	0.082	11.7	2.4	2.1	7.51
(483-20-1p13a)	169	100–375	8	28	24.9	0.025	2.0	2.2	4.0	6.01
(483-20-1p13b)	169	200–425	8	40	14.4	0.029	2.5	3.9	6.9	8.58
483-21-1p6a	178	200–375	5	35	19.9	0.018	2.0	1.4	8.2	7.51
483-21-1p6b	178	100–300	5	38	15.8	0.032	1.5	5.2	3.8	8.15
483-21-2p8b	179.5	200–375	5	59	6.3	0.056	4.6	1.9	3.8	12.65
483-21-3p1a	181	200–375	6	23	4.6	0.075	7.6	8.0	5.9	4.93
483-23-1p8ab	187	350–525	8	48	18.6	0.029	2.5	0.4	2.0	10.29
483-23-2p8aa	188.5	375–525	7	50	7.4	0.050	8.8	2.1	1.1	10.72
*483b-12-1p1a	169	150–350	6	9	12.1	0.028	7.1	5.4	10.5	1.93
*483b-21-2p1a	213	400–500	5	4	5.3	0.056	5.9	2.1	7.3	0.85
483b-22-1p1ab	217.5	200–400	7	5	6.1	0.069	13.6	5.9	10.3	1.07
483b-22-2p3b	219	250–450	8	33	12.2	0.038	6.3	3.1	5.7	7.08
483b-22-2p7cb	219	100–250	4	30	6.1	0.075	4.1	1.7	1.7	6.43
483b-29-1p2ba	249	250–400	5	15	3.3	0.077	7.0	13.0	4.1	3.21
*483b-32-3p7a	262.5	400–550	7	5	23.3	0.021	4.9	4.0	4.4	1.07

A list of the complete data set is available at ftp://sorcerer.ucsd.edu/pub/data/sbg98. Specimen names are the DSDP piece identifications (see text). Depth is the depth in meters below sea floor of the top of the core section in which the specimen was found. T_{min}–T_{max} are temperature bounds used for the calculation. N is the number of steps. B is the ancient field in μT estimated from the data. Q is the quality factor [13]. σ/|b| is the scatter about the best-fit line (see text). MAD is the maximum angular deviation [20] of the remanence data through the interval used in the calculation. α is the angle between the resultant vector of the same data and the principle component (see text). DRAT is the difference ratio (see text). VADM is the VADM (10^{22} Am^2) calculated for each field estimate using the latitudes in Table 2. Grade A data meet the following criteria: DRAT < 10%, σ/|b| < 0.1, α < 15, MAD < 15. Specimens in parentheses were eliminated from the calculation of the averages and specimens with * have a duplicate grade B specimen with a concordant estimate of B.

same cooling unit. Arai plots from examples of data from duplicate chips that both were given grades of 'A' are shown in Fig. 3.

Most duplicate specimens yield field estimates within a few μT of one another; most are much better than the 15% criterion used for culling the Montpellier database. An example of a pair of specimens in this study that failed to give concordant results is shown in Fig. 3d. One specimen suggests a paleofield of 28 μT while the other suggests 48 μT. Both specimens passed all acceptance criteria, yet the result is clearly unreliable. While only five specimens from this study have replicate grade A results (see Table 3), another

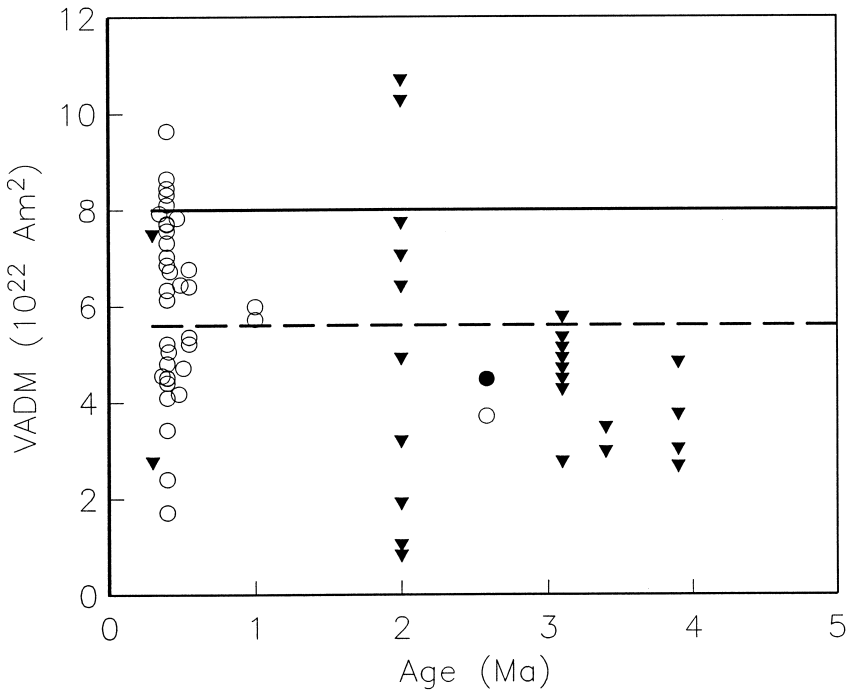

Fig. 4. Open symbols are data from the published literature that were obtained with a Thellier–Thellier experiment that used pTRM checks (see text and Table 1). The solid triangles are the chilled margin averages of data from Table 3 (see text). The dashed line is the average field value calculated from these data and the solid line is the value of the axial dipole moment from the 1995 International Geomagnetic Reference Field [5].

six have concordant grade B sisters. These are marked with asterisks in Table 3.

Discordant behavior among sister specimens is rare in our experience with SBG. We estimate that approximately 5% of our results fall into this category.

4. Results and discussion

In order to make paleofield estimates by cooling unit, we first take the arithmetic average of any multiple specimens from a given chilled margin. We eliminated the one case marked by parentheses in Table 3 which gave discordant results between two sister specimens.

The VADMs in Table 3 range from less than one to nearly 13×10^{22} Am^2 with a mean of $4.89\pm2.86\times10^{22}$ Am^2, virtually identical to the time-averaged field predicted by Coe [4]. The entire range of the data is represented at Site 483, for which there are the most data. Although it is likely that a given drill core sampled the same margin more than once, it is impossible to establish this in any given case. Therefore, for the purposes of this discussion, we will assume that each chilled margin represents a discrete cooling unit. Most sites yielded few specimens and the mean value does not constitute an average value. Therefore, we treat the data set as a whole and attempt to calculate the time-averaged intensity of the geomagnetic field for the period of time 0.3–5 Ma.

We plot VADM data from Table 1 (open symbols) and Table 3 (closed symbols) (averaged by chilled margin) in Fig. 4. These data are also shown in a quantile–quantile plot (see [15] for a discussion of quantile–quantile plots in paleomagnetism) against the trend expected from a normal distribution in Fig. 5. The general linearity of the plot suggests that the data are drawn from a normal distribution hypothesis supported by the fact that the so-called D statistic does not exceed the

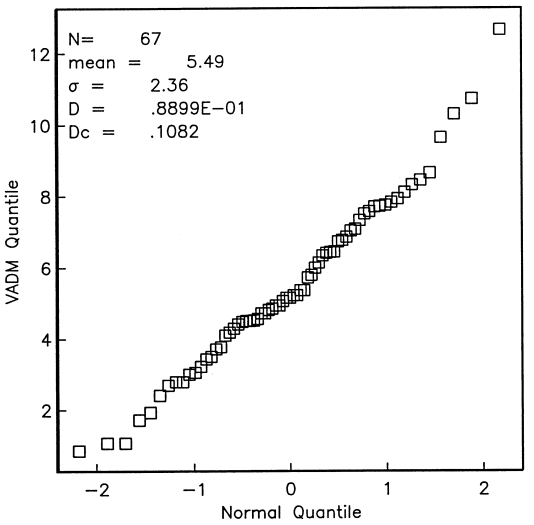

Fig. 5. Quantile–quantile plot of VADM data from Tables 1 and 3. The general linearity of the plot suggests that the data are drawn from a normal distribution, a contention supported by the fact that the D statistic is lower than D_c, suggesting that the data are normally distributed (with a certainty of better than 95%).

critical value D_c at the 95% level of certainty. Based on this, we calculate an arithmetic mean for the data, as opposed to a geometric mean. The arithmetic mean for the data shown in Fig. 4 and Tables 1 and 3 is $5.49 \pm 2.36 \times 10^{22}$ Am^2, substantially lower than the oft-quoted average value of approximately 8×10^{22} (e.g. [2,3,21]).

As shown in Fig. 1, inclusion of lower quality data leads to higher average values of the geomagnetic field. Goguitchaichvili et al. [3] found that if a proper Thellier–Thellier experiment was performed, the reported high field values during a paleomagnetic transition in Iceland [22] could not be duplicated and that all the high field values were associated with lava flows that had a poor performance of the pTRM checks. It appears that errors are not random in experiments that do not include the pTRM checks, but systematically biased too high. Possible causes of a bias to high field estimates are viscous remanence in normal specimens and misinterpretation of the curved slope caused by multi-domain magnetizations (see [4]). The latter is particularly prevalent in more slowly cooled lava flows that have larger grain sizes. Viscous remanences are usually removed by demagnetization to a few hundred degrees and most researchers do not interpret the initial steep slope in the Arai plot as the primary TRM. However, in the Shaw method, VRM is difficult to detect and could well contribute to the NRM, biasing the paleofield estimate toward higher values. The multi-domain effect produces a curved Arai plot, or one with several line segments. These data all pass pTRM checks, distinguishing this phenomenon from alteration during laboratory heating, which often also produces a break in slope in the Arai plot (see for example Fig. 3c, circles). Alteration during laboratory heating can be detected by failed pTRM checks (as in Fig. 3c). This is a well known effect, so researchers performing Thellier experiments without pTRM checks might shy away from the last slope on the assumption that it was an artifact of alteration, choosing instead a steeper slope. If this was instead a multi-domain effect, the result would be a field estimate that was too high. Without the full T+ experiment, therefore, there is a tendency to err systematically to higher estimates of the paleofield.

5. Conclusions

(1) The average value of the paleointensity of the geomagnetic field for the period 0.3–5 Ma is some 5.5×10^{22} Am^2, substantially lower than the oft-quoted value of 8×10^{22} Am^2 [2]. The present field is therefore anomalously strong.
(2) Our average is based on both 'traditional' paleointensity materials (e.g. lava flows) in the published data base as well as the relatively 'new' approach of using SBG. The low field estimate therefore is not an artifact of the use of glass, but is a robust estimate based on the highest quality data available.
(3) There is a systematic bias in paleointensity data obtained without a Thellier–Thellier experiment that includes pTRM checks.

Acknowledgements

We thank the hospitality of Fort Hoofddijk, in

particular, Cor Langereis, for allowing this project to go on in their midst. We also acknowledge many useful discussions with Jeff Gee, Cathy Constable and Peter Selkin. Thom Pick greatly facilitated this project in its early stages. Reviews by M. Perrin, M. Prévot, S. Levi, W. Zhou and one anonymous reviewer greatly improved the manuscript. This work was supported by funds from GOA and the NSF.*[RV]*

References

[1] T. Juarez, L. Tauxe, J.S. Gee, T. Pick, The intensity of the Earth's magnetic field over the past 160 million years, Nature 394 (1998) 878–881.
[2] P. McFadden, M.W. McElhinny, Variations in the geomagnetic dipole 2: statistical analysis of VDM's for the past 5 m.y., J. Geomagn. Geoelectr. 34 (1982) 163–189.
[3] A.T. Goguitchaichvili, M. Prévot, P. Camps, No evidence for strong fields during the R3-N3 Icelandic geomagnetic reversal, Earth Planet. Sci. Lett. 167 (1999) 15–34.
[4] R.S. Coe, Paleointensities of the Earth's magnetic field determined from Tertiary and Quaternary rocks, J. Geophys. Res. 72 (1967) 3247.
[5] C.E. Barton, R.T. Baldwin, D.R. Barraclough, S. Bushati, M. Chiappini, Y. Cohen, R. Coleman, G. Hulot, P. Kotze, V.P. Golovkov, A. Jackson, R.A. Langel, F.J. Lowes, D.J. McKnight, S. Macmillan, L.R. Newitt, N.W. Peddie, J.M. Quinn, T.J. Sabaka, International geomagnetic reference field, 1995 revision, Geophys. J. Int. 125 (1996) 318–321.
[6] J. Gee, D.A. Schneider, D.V. Kent, Marine magnetic anomalies as recorders of geomagnetic intensity variations, Earth Planet. Sci. Lett. 144 (1996) 327–335.
[7] J.P. Valet, L. Meynadier, Geomagnetic field intensity and reversals during the past four million years, Nature 366 (1993) 234–238.
[8] G.A. Glatzmaier, P.H. Roberts, Simulating the geodynamo, Cont. Phys. 38 (1997) 269–288.
[9] G.A. Glatzmaier, R.S. Coe, L. Hongre and P.H. Roberts (1999) How the Earth's mantle controls the frequency of geomagnetic reversals, Nature (submitted).
[10] M. Prévot, M.E.M. Derder, M. McWilliams, J. Thompson, Intensity of the Earth's magnetic field: evidence for a Mesozoic dipole low, Earth Planet. Sci. Lett. 97 (1990) 129–139.
[11] E. Thellier, O. Thellier, Sur l'intensité du champ magnétique terrestre dans le passé historique et geologique, Ann. Geophys. 15 (1959) 285–378.
[12] R.S. Coe, The determination of paleointensities of the Earth's magnetic field with emphasis on mechanisms which could cause non-ideal behavior in Thellier's method, J. Geomagn. Geoelectr. 19 (1967) 157–178.
[13] R.S. Coe, S. Grommé, E.A. Mankinen, Geomagnetic paleointensities from radiocarbon-dated lava flows on Hawaii and the question of the Pacific nondipole low, J. Geophys. Res. 83 (1978) 1740–1756.
[14] M. Perrin, E. Schnepp, V. Shcherbakov, Paleointensity database updated, EOS 79 (1998) 198.
[15] L. Tauxe, Paleomagnetic Principles and Practice, Modern Approaches in Geophysics, Kluwer Academic Publishers, Amsterdam, 1998.
[16] J. Shaw, A new method of determining the magnitude of the paleomagnetic field application to five historic lavas and five archeological samples, Geophys. J. R. Astron. Soc. 39 (1974) 133–141.
[17] S.C. Cande, D.V. Kent, Revised calibration of the geomagnetic polarity timescale for the late, J. Geophys. Res. 100 (1995) 6093–6095.
[18] L. Tauxe, T.A.T. Mullender, T. Pick, Potbellies, wasp-waists, and superparamagnetism in magnetic hysteresis, J. Geophys. Res. 101 (1996) 571–583.
[19] T. Pick, L. Tauxe, Holocene paleointensities: Thellier experiments on submarine basaltic glass, J. Geophys. Res. 98 (1993) 17949–17964.
[20] J.L. Kirschvink, The least-squares line and plane and the analysis of paleomagnetic data, Geophys. J. R. Astron. Soc. 62 (1980) 699–718.
[21] H. Tanaka, M. Kono, S. Kaneko, Paleosecular variation of direction and intensity from two Pliocene-Pleistocene lava sections in southwestern Iceland, J. Geomagn. Geoelectr. 47 (1995) 89–102.
[22] J. Shaw, Strong geomagnetic fields during a single Icelandic polarity transition, Geophys. J. R. Astron. Soc. 40 (1975) 345–350.
[23] H. Otake, H. Tanaka, M. Kono, K. Saito, Paleomagnetic study of Pleistocene lavas and dykes of the Zao volcano group, Japan, J. Geomagn. Geoelectr. 45 (1993) 595–612.
[24] E. Schnepp, H. Hradetzky, Combined paleointensity and $^{40}Ar/^{39}Ar$ age spectrum data from volcanic rocks of the West Eifel field (Germany): evidence for an early Brunhes geomagnetic excursion, J. Geophys. Res. 99 (1994) 9061–9076.
[25] E. Schnepp, Paleointensity study of Quaternary East Eifel phonolitic rocks (Germany), Geophys. J. Int. 121 (1995) 627–633.
[26] E. Schnepp, Geomagnetic paleointensities derived from volcanic rocks of the Quaternary East Eifel volcanic field, Germany, Phys. Earth Planet. Int. 94 (1996) 23–41.